Journal of Alloys and Compounds 509 (2011) 6196–6199

Contents lists available at ScienceDirect

Journal of Alloys and Compounds

journal homepage: www.elsevier.com/locate/jallcom

Photosensitive nanostructured TiO_2 grown at room temperature by novel "bottom-up" approached CBD method

U.M. Patil, S.B. Kulkarni, P.R. Deshmukh, R.R. Salunkhe, C.D. Lokhande*

Thin Film Physics Laboratory, Department of Physics, Shivaji University, Kolhapur 416 004, India

ARTICLE INFO

Article history:
Received 24 December 2010
Received in revised form 12 February 2011
Accepted 16 February 2011
Available online 23 February 2011

Keywords:
Thin film
Titanium dioxide (TiO_2) nanostructure
Chemical synthesis
Optical properties
Photoresponse

ABSTRACT

The current paper incorporates with a "bottom-up" approached chemical bath deposition method to grow titanium dioxide (TiO_2) nanostructure at room temperature on glass and stainless steel substrates. The room temperature deposited TiO_2 films are heat treated at 673 K for 1 h in air and the corresponding change in structural, morphological and optical properties are studied by means of X-ray diffraction (XRD), Fourier transform infrared (FTIR), scanning electron microscopy (SEM), and UV–VIS–NIR spectrophotometer. The heat-treated films are utilized as a photocathode in photoelectrochemical (PEC) cell in 1 M NaOH electrolyte. The experimental results show that, the CBD method allows formation of photosensitive, anatase TiO_2 thin film, which can be potentially tuned in many functional applications with feasibility.

1. Introduction

The assemblies of low-dimensional building blocks (nanodots, nanowires, nanobelts, nanotubes, etc.) into hierarchical architectures on various substrates have great interest because of the demands for many practical applications in functional devices [1]. As one of the most important oxide semiconductor materials, TiO_2 has attracted considerable attention due to its good optical, electrical, and photoelectrochemical (PEC) properties [2–4]. Various quasi-one-dimensional nanostructures of TiO_2 have been grown, including nanoparticles; nanorods, nanotubes, etc., by several "bottom-up" processes such as hydrothermal growth, sol–gel, anodization of Ti substrate, and chemical deposition methods [5–9]. Interconnected nanoflakes surface is one such morphology which has attracted increasing interest due to distinctive morphology, large surface area and high aspect ratio [10].

To synthesize nanomaterials various methods are under consideration, which are divided in to two approaches. The nanomaterials can either built from separate atoms (an approach from the "bottom-up") or by various dispersion and aggregation (an approach from the "top-down"). The approach from the "bottom-up" largely pertains to chemical methods including chemical bath deposition (CBD), successive ionic adsorption and reaction, electrodeposition, sol––gel, hydrothermal growth, etc., for preparation of nanosize particles whereas physical methods are approaches from "top-down" like sputtering, vacuum evaporation, etc. deposition techniques. CBD is one of the "bottom-up" process, has been well developed to fabricate large-area semiconductor thin films in view of its several advantages: it does not require sophisticated instruments; the starting chemicals are commonly available and cheap; the preparation parameters are easily controlled [11,12]. However, little work has been done to prepare dense and adherent TiO_2 films by CBD method [13–15]. In order to improve the physical and chemical performance in the devices, designing the morphology of TiO_2 is a focus of current research.

On the basis of the above discussion, the present study is paying attention to the synthesis of TiO_2 nanostructure contains with nanoflakes. In the present paper, we report for the first time, a "bottom-up" process for TiO_2 nanoflakes at room temperature by CBD method.

2. Experimental

The TiO_2 nanoflakes were synthesized at room temperature by "bottom-up" approach using CBD method. Room temperature deposition avoids oxidation and corrosion of metallic substrates. Chemical deposition results in pin hole free and uniform deposits are easily obtained since the basic building blocks are ions instead of atoms. Preparative parameters such as pH of solution, deposition time, and concentration of precursor were optimized. In the typical synthesis, equimolar (0.1 M) titanium trichloride ($TiCl_3$, 30% HCl) and ammonium chloride (NH_4Cl) in total 100 mL double distilled water is used as reacting bath. The ultrasonically cleaned glass and stainless steel substrate dipped vertically in the reaction bath. The depositions were carried out at predetermined time interval in between 15 and 35 h. White colored TiO_2 films were carried out on the ultrasonically cleaned substrates. In order to remove hydroxide from deposited film and to improve the crystallinity the films were heat treated at 673 K for 1 h.

* Corresponding author. Tel.: +91 231 2609229.
E-mail address: l.chandrakant@yahoo.com (C.D. Lokhande).

0925-8388/$ – see front matter © 2011 Elsevier B.V. All rights reserved.
doi:10.1016/j.jallcom.2011.02.091

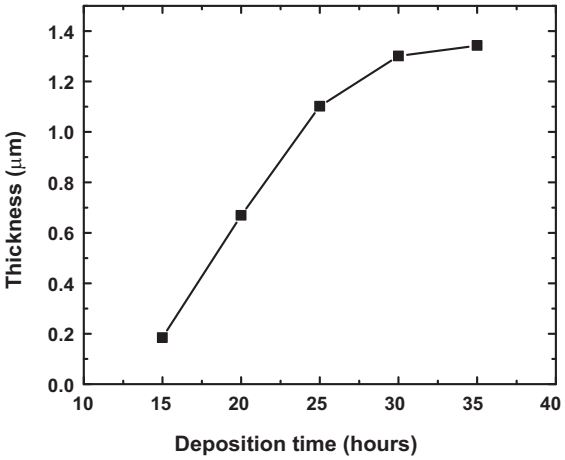

Fig. 1. Variation of TiO_2 film thickness with deposition time.

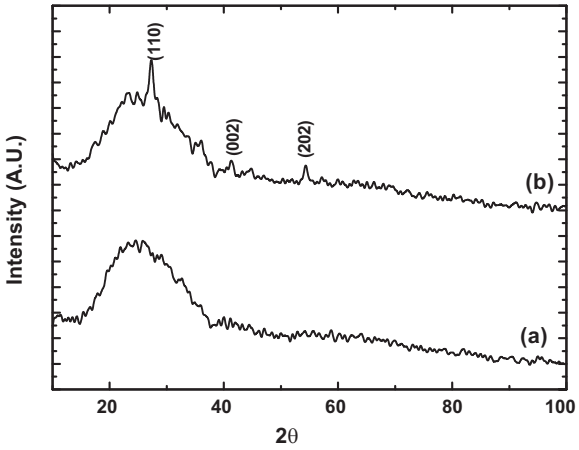

Fig. 2. X-ray diffractograms of (a) as-deposited and (b) heat-treated at 673 K of TiO_2 thin films.

Crystallographic study was carried out using Phillips PW-1710, X-ray diffractometer using Cu Kα radiation in the 2θ range from 20 to 100°. FT-IR spectra of the samples were collected using a 'Perkin Elmer, FT-IR Spectrum one' unit. The surface morphology was visualized using a JEOL-6360 scanning electron microscope (SEM). Optical absorption spectra were recorded over the wavelength range 300–900 nm using UV–VIS–NIR spectrophotometer Systronics-119. Photoresponse was studied by forming a cell comprising heat treated TiO_2 (on stainless steel substrate) as a photocathode, graphite as counter electrode and saturated calomel electrode (SCE) as a reference electrode in the 1 M NaOH electrolyte.

3. Results and discussion

3.1. Reaction mechanism

CBD method is based on the formation of solid phase from a solution, which involves two steps as the nucleation and particle growth. The growth kinetics of a thin film deposition process is ion-by-ion growth mechanism, which involves the ion-by-ion deposition at nucleation sites on the immersed surfaces [16].

For deposition of TiO_2 films, $TiCl_3$, 30% HCl was used as a source of titanium and ammonium chloride as a complexing agent. At the beginning of reaction:

$$NH_4Cl \rightarrow NH_4^+ + Cl^- \quad (1)$$

$$NH_4^+ + OH^- \leftrightarrow NH_3 \cdot H_2O \quad (2)$$

Ti^{3+} cations form amine complex of $Ti(NH_3)n^{3+}$ ($n = 1$–4) with NH_3 (aq) in solution as:

$$Ti^{3+} + nNH_3 \rightarrow Ti(NH_3)n^{3+} \quad (3)$$

Here, initially the solution is acidic and the pH value is about 1 and then the pH of solution increases gradually and monotonically with time and the solution becomes alkalescent. At this alkalescent bath condition, the $Ti(NH_3)n^{3+}$ is unstable and the following reactions occur:

$$Ti(NH_3)n^{3+} \leftrightarrow Ti^{3+} + nNH_3 \quad (4)$$

$$Ti^{3+} + nH_2O \rightarrow Ti(OH)_3^+ \quad (5)$$

$$Ti(OH)_3^+ + OH^- \rightarrow TiO_2 + 2H_2O \quad (6)$$

When the deposition is finished, pH value decreases again owing to the consumption of OH^-. In the processing, the ammonium chloride is introduced as a complexing agent and exerts itself to control the release velocity of Ti^{3+} ions for deposition of TiO_2 thin film.

Fig. 1 shows the graph of TiO_2 film thickness variation with deposition time. Nonlinear rate of increase in the thickness attributed to the growth by nucleation and coalescence process. More nucleation sites contribute to coagulation during the growing procedure. Furthermore, slight decrease in thickness attributed to the formation of outer porous layer and/or the film which may have developed stress which tends to cause delamination, resulting in peeling off the film [17].

3.2. Structural characterization

Fig. 2(a) and (b) shows typical X-ray diffraction patterns of as-deposited and heat-treated TiO_2 thin films on glass substrate (with 1.3 μm film thickness). The X-ray diffractogram of as-deposited film reveals the amorphous nature of the film. After heat treatment, TiO_2 shows poorly crystalline structure with less intense peak corresponds to (1 0 0), (0 0 2) and (2 0 2) in consistent with anatase phase [JCPDS card no. 21-1276].

3.3. FTIR studies

The IR absorption spectra of as-deposited and heat treated TiO_2 powder in the range 4000–400 cm^{-1} are shown in Fig. 3. The four sharp absorption bands at ν_1: 612, ν_2: 950, ν_3: 1631 and ν_4: 3500 cm^{-1} are attributed to the stretching vibration of Ti–O–Ti in anatase, peroxo group, vibration of hydroxyl groups of molecular water and stretching vibrations of OH, respectively [18,19]. This result indicated that, as deposited film contained hydroxide and other bonds, which indicates that formation of hydroxide that cannot be avoided in the CBD method. After heat treatment, the peak corresponds to OH groups were decreases. Less intense hydroxide

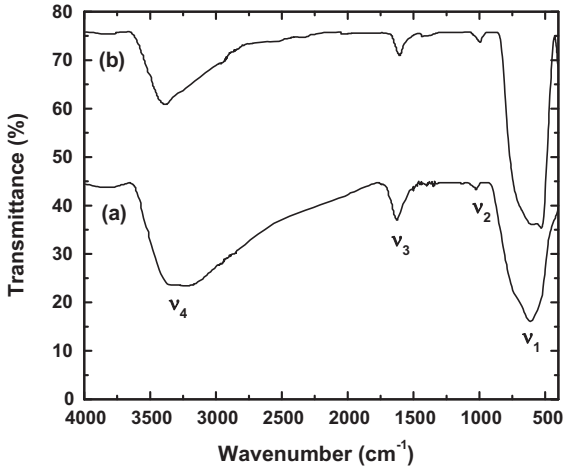

Fig. 3. FTIR spectra of (a) as-deposited and (b) heat treated TiO_2 films.

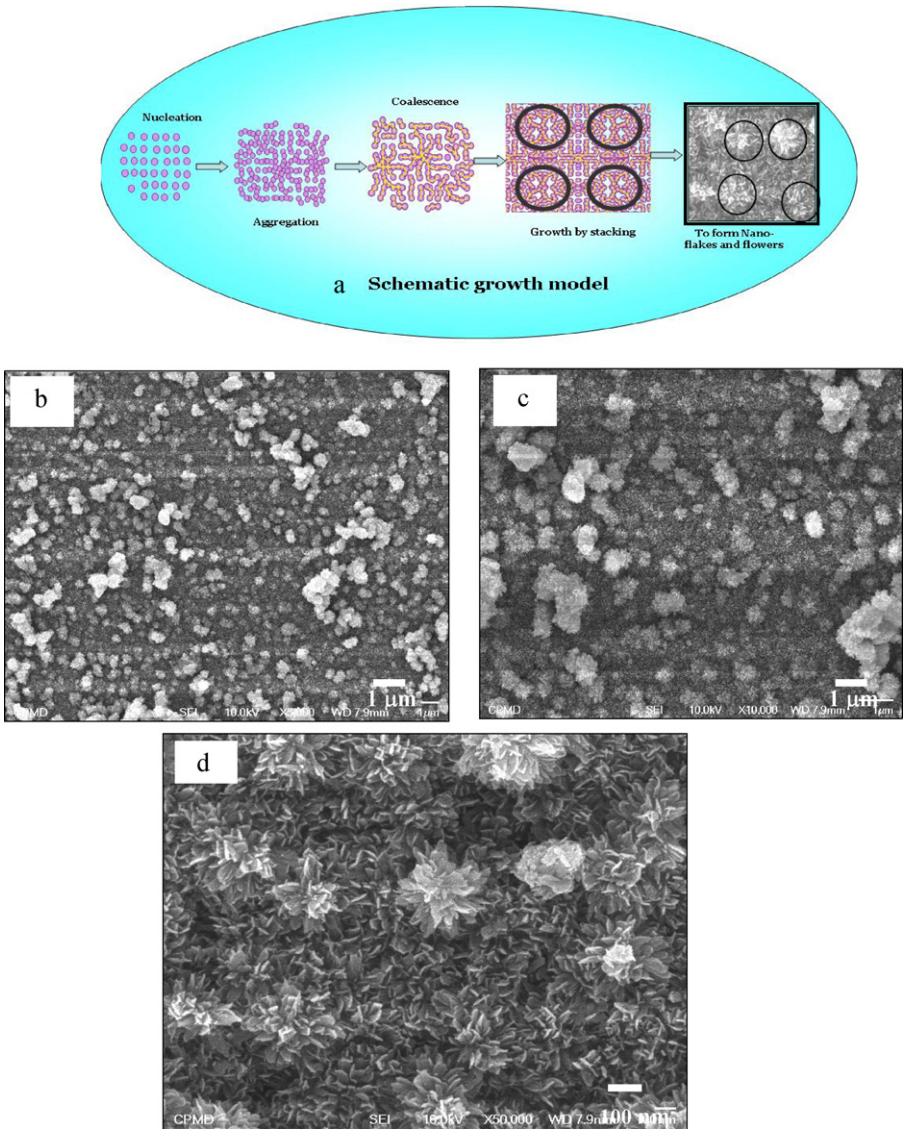

Fig. 4. (a) Schematic growth model for TiO_2 nanoflakes. The SEM micrographs (10,000×) of (b) as-deposited and (c) heat treated TiO_2 film. (d) High magnification (50,000×) SEM micrograph of heat treated TiO_2 film.

and hydroxyl groups from water found in the heat treated TiO_2 may be due to the fact that the spectra were not recorded in situ and some adsorption of water from the ambient atmosphere has occurred.

3.4. Surface morphology

The schematic growth model for TiO_2 nanoflakes is shown in Fig. 4(a). Chemical bath deposition is one of the "bottom-up" approach method based on the formation of a solid phase upon transformation of a supersaturated solution to the saturated state. This transformation incorporated with various distinct steps as nucleation, aggregation, coalescence and subsequent growth by stacking of the particles. During nucleation, clusters of metal precursor molecules likely undergo rapid decomposition. Such nucleation centers acted as foundation for the aggregation of the particles. Moreover, basic groundwork for the nanostructure is formed by coalescence of aggregated particles. Subsequently, the film grows to a certain thickness on the substrate surface by stacking of the particles [20].

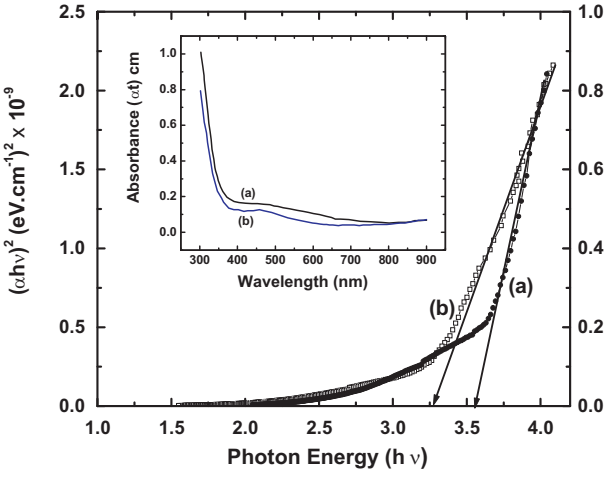

Fig. 5. Plot of $(\alpha h\nu)^2$ vs. energy $h\nu$ of (a) as-deposited and (b) heat-treated TiO_2 films. Inset shows variation of absorption (αt) with wavelength (λ) of (a) as-deposited and (b) heat-treated TiO_2 films on glass substrate.

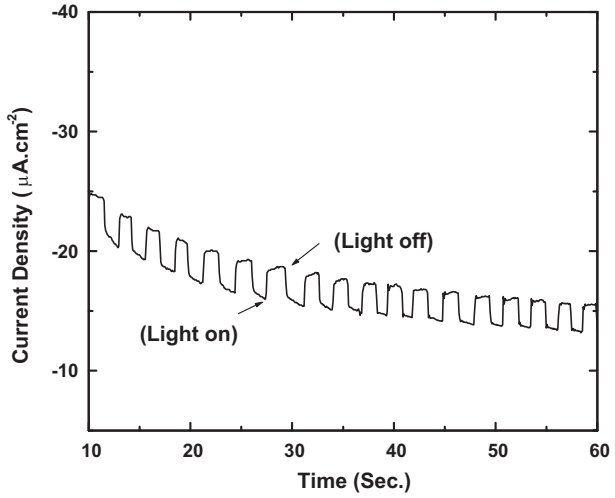

Fig. 6. Current–time characteristic of heat-treated TiO_2 film at −0.1 V by chronoamperometry under illumination of white light (100 mW/cm^2).

Fig. 4(b) and (c) shows the surface morphology (at 10,000× magnification) of as-deposited and heat-treated TiO_2 films. From the micrographs, one can see the total coverage of the substrate with the of TiO_2 nanoflakes. As-deposited, small nanoflakes growth is favored on the substrate surface. Conversely, as an effect of heat treatment the diffusion rate of the constituent atoms is high resulting in a high rate of formation of TiO_2 larger nanoflakes. Fig. 4(d) shows the typical SEM image of heat treated TiO_2 sample with 50,000× magnification, which reveals that the flower-shaped TiO_2 is not a simple aggregation of small crystallites, but is composed by nanoflakes growing homocentrically. The flakes are typically of few nanometers in thickness and tens of nanometers in dimension. The TiO_2 flakes lie on but do not grow on the substrates. TiO_2 nanoflakes may demonstrate high performance levels for PEC application because of their increased surface area.

3.5. Optical studies

For the purpose of the absorption study, TiO_2 film with less thickness (0.6 μm) is used. Inset of Fig. 5 shows the variation of optical absorbance (αt) of as-deposited and heat-treated TiO_2 thin films with wavelength (λ). A quick inclining trend of spectrum in regime 300–400 nm was observed. The optical absorption spectrum of TiO_2 film on glass substrate showed a sharp increase in absorption below 350 nm with a tailing absorbance in the 400–500 nm was observed. Lokhande et al. reported similar nature of absorbance for the TiO_2 thin films [13]. Such tailing absorption attributed to the presence of an electronic band due to defects states close to the conduction band for sub-stoichiometric TiO_2 material [21]. The absorption spectra of the nanocrystalline TiO_2 show shift towards the higher wavelength after heat treatment (red shift) with increasing grain size and is attributed to quantum size effects [22]. The high optical absorption coefficient (10^4 cm^{-1}) indicates that the TiO_2 thin film have direct band-gap transition. The absorbance data was further used to calculate the direct band gap energy of the TiO_2 thin films:

$$\alpha = \frac{A(h\nu - E_g)^n}{h\nu} \quad (7)$$

Fig. 5 presents the plot of $(\alpha h\nu)^2$ against $h\nu$ for both TiO_2 films. The good relation between $(\alpha h\nu)^2$ versus $h\nu$ implies the direct transition nature for TiO_2 films. For as deposited and heat treated TiO_2 films, a band gap 3.54 and 3.26 eV, respectively, was obtained. Decrease in band gap energy after heat treatment is attributed to increase in flower size with flake size. This opens up the possibility of the constructing thin film devices from these nanoflakes with tunable optical properties.

3.6. Photoelectrochemical (PEC) response

The PEC response under chopped light (100 mW/cm^2) conditions carried out in order to study the photosensitivity of the TiO_2 nanoflakes. Photoresponse of heat treated TiO_2 nanoflakes was carried out by forming a typical TiO_2 (steel substrate)/1 M NaOH/graphite cell. Fig. 6 shows the current–time characteristic of TiO_2 film at −0.1 V in potentiostatic mode. The photocurrent is obtained of the order of μA cm^{-2}. The low photocurrents have been attributed to high band gap (>3.2 eV) and almost amorphous structure (as evidenced by XRD studies) of TiO_2 films. Fig. 6 shows rapid changes in the photocurrent upon the beginning and at the end of illumination. Nelson et al. [23] showed that this behavior could be explained by a model considering photogeneration, trapping and scavenging of electrons, where the photogeneration rate was found to be responsible for the photocurrent rise.

4. Conclusions

In summary, TiO_2 nanoflakes like morphology have been controllably synthesized by the CBD method with NH_4Cl as complexing agent. The XRD and FTIR studies confirm the formation of anatase TiO_2 thin film. SEM images reveal the improvement in flower size of TiO_2 as an effect of heat treatment. The strong influence of wide band gap of this electrode in spite this, PEC performance can motivate to check its feasibility in DSSC's devices. The CBD method is constructive for preparation of large area nanoflaked TiO_2 electrodes for PEC cells at the expense of small amount of initial ingredients.

Acknowledgement

UMP is thankful to UGC-New Delhi for financial support through UGC-Research Fellowship for meritorious student.

References

[1] Y. Huang, X.F. Duan, Y. Cui, L.J. Lauhon, K.H. Kim, C.M. Lieber, Science 294 (2001) 1313.
[2] A. Yamakata, T. Ishibashi, H. Onishi, J. Mol. Catal. A: Chem. 199 (2003) 85.
[3] B. O'Regan, M. Gratzel, Nature 335 (1991) 737.
[4] L. Kavan, A. Attia, F. Lenzmann, S.H. Elder, M. Gratzel, J. Electrochem. Soc. 147 (2000) 2897.
[5] X.M. Sun, Y.D. Li, Chem. Eur. J. 9 (2003) 2229.
[6] S.J. Bu, Z.J. Jin, X.X. Liu, L.R. Yang, Z.J. Cheng, J. Eur. Ceram. Soc. 25 (2005) 673.
[7] G.K. Mor, O.K. Varghese, M. Paulose, G.A. Grimes, Adv. Funct. Mater. 15 (2005) 1291.
[8] B.R. Sankapal, M.C. Lux-Steiner, A. Ennaoui, Appl. Surf. Sci. 239 (2005) 165.
[9] S.S. Kale, R.S. Mane, Hoeil-Chung, M.-Y. Yoon, C.D. Lokhande, S.-H. Han, Appl. Surf. Sci. 253 (2006) 421.
[10] H. Wang, C. Xie, J. Cryst. Growth 291 (2006) 187.
[11] R.S. Mane, C.D. Lokhande, Mater. Chem. Phys. 65 (2000) 1.
[12] C.D. Lokhande, Mater. Chem. Phys. 27 (1991) 1.
[13] C.D. Lokhande, E.-H. Lee, K.-D. Jung, O.-S. Joo, J. Mater. Sci. Lett. 39 (2004) 2915.
[14] R.S. Mane, Y.H. Hwang, C.D. Lokhande, S.D. Sartale, S.-H. Han, Appl. Surf. Sci. 246 (2005) 271.
[15] H.M. Pathan, W.Y. Kim, K.-D. Jung, O.-S. Joo, Appl. Surf. Sci. 246 (2005) 72.
[16] G. Hodes, Chemical Solution Deposition of Semiconductor Films, Marckel Dekkar, Inc., New York, 2002, p. 40.
[17] J.A. Thorton, J. Vac. Sci. A24 (1986) 3056.
[18] A.N. Josea, J.T. Juan, D. Pablo, R.P. Javier, R. Diana, I.L. Marta, Appl. Catal. A: Gen. 178 (1999) 191.
[19] Y. Wang, N. Herron, J. Phys. Chem. 95 (1991) 525.
[20] V.R. Shinde, C.D. Lokhande, R.S. Mane, S.H. Han, Appl. Surf. Sci. 245 (2005) 407.
[21] I. Justica, P. Ordejon, G. Canto, J.L. Mozes, J. Fraxedas, G. Abattiston, R. Gerbasi, A. Figueras, Adv. Mater. 14 (2002) 1399.
[22] C. Kormann, D.W. Bahnemann, M.R. Hoffmann, J. Phys. Chem. 92 (1988) 5196.
[23] J. Nelson, A.M. Eppler, I.M. Ballard, J. Photochem. Photobiol. A: Chem. 148 (2002) 25.